Ceramics International 46 (2020) 1178–1182

Contents lists available at ScienceDirect

Ceramics International

journal homepage: www.elsevier.com/locate/ceramint

Up-conversion luminescence of $LiTaO_3:Er^{3+}$ phosphors for optical thermometry

Xin Yang[a], Shaopeng Lin[b], Decai Ma[b], Siwei Long[a], Yunzhong Zhu[b], Huashan Li[a,*], Biao Wang[a,b,**]

[a] School of Physics, Sun Yat-sen University, Guangzhou, 510275, China
[b] Sino French Institute of Nuclear Engineering and Technology, Sun Yat-sen University, Zhuhai, 519082, China

ARTICLE INFO

Keywords:
$LiTaO_3:Er^{3+}$
Phosphors
Fluorescence intensity ratio
Optical thermometry

ABSTRACT

We synthesized $LiTaO_3:Er^{3+}$ phosphors by molten salt method, and systematically investigated their phase structure, micro-morphology, up-conversion luminescence, and optical temperature sensing properties. The up-conversion luminescence was demonstrated to arise from two near-infrared photon absorption process, which can be optimized by tuning Er^{3+} dopant concentration. The corresponding mechanism was proposed based on the transitions between dopant states as illustrated in an energy level diagram. The optical temperature sensing properties were explored by utilizing the fluorescence intensity ratio method. Notably, a wide operation scope ranging from 100 to 500 K was obtained, along with a relatively large energy gap ($\Delta E = 698\ cm^{-1}$) and a high absolute sensitivity ($S_a = 3.34 \times 10^{-3}\ K^{-1}$ at 492 K). The impressive properties of $LiTaO_3:Er^{3+}$ phosphors in combination with the incomparable multifunctional feature of host material reveal their potential for developing integratable up-conversion optical thermometry.

1. Introduction

In recent years, optical thermometry has evoked wide attentions in scientific research and advanced manufacturing because of its outstanding features of non-contact, enhanced sensitivity and high measurement accuracy [1–5]. Generally, optical thermometry bases on the fluorescence intensity ratio (FIR), which is obtained through comparing two thermally coupled levels (TCLs) stemming from one kind of active ions. Up-conversion luminescence (UCL), reported as a promising optical thermometry strategy [1,3,6,7], refers to the phenomenon of converting more than two absorbed low energy photons to a high energy photon emitting subsequently. Rare earth (RE) ions (Nd^{3+}, Er^{3+}, Ho^{3+}, Tm^{3+}, Eu^{3+}, Sm^{3+}) doped phosphors have been extensively investigated for UCL based optical thermometry, benefited from their remarkable variation of FIR with temperature [1,8–11]. Among various RE ions, Er^{3+} possesses a set of TCLs ($^2H_{11/2}$ and $^4S_{3/2}$) with an energy gap around $800\ cm^{-1}$, rendering most of the Er^{3+} doped matrixes highly suitable as optical thermometers [12–14]. The relatively cheap price of 980 nm laser diode as the excitation source also enables the construction of low-cost and integrable systems. The temperature dependences of FIR have been reported for Er^{3+} doped phosphors based on various host materials, including Sr_2YbF_7 Glass-Ceramics [15], CaZnOS multifunctional piezoelectric semiconductor [16], silicate glass [17], germanate glasses [18], Al_2O_3 [19], ZnO [20], and $SrSnO_3$ [21] *etc*.

The desirable optical properties and high compatibility with various matrix of Er^{3+} doped materials unveil its potential applications in integrated optics, which aims to create miniature optical circuits similar to the silicon chips [22]. Developing novel hosts materials, that makes the optical thermometer compatible with a variety of light-controlling components integrated into a single chip, is essential to realize such promise.

Lithium tantalate ($LiTaO_3$, LT) is a well-known multifunctional host material for integrated optics because of its excellent ferroelectric, piezoelectric, acousto-optical, electro-optical, and nonlinear optical properties, along with high mechanical and chemical stabilities [23–25]. Although their photoluminescence properties have been carefully studied [26–28], exploitation of LT matrix as the building block of optical thermometer has not been reported yet.

In this work, series of $LiTaO_3:Er^{3+}$ phosphors were synthesized

* Corresponding author.
** Corresponding author. School of Physics, Sun Yat-sen University, Sino French Institute of Nuclear Engineering and Technology, Sun Yat-sen University, Zhuhai, 519082, China.
E-mail addresses: lihsh25@mail.sysu.edu.cn (H. Li), wangbiao@mail.sysu.edu.cn (B. Wang).

https://doi.org/10.1016/j.ceramint.2019.09.088
Received 24 July 2019; Received in revised form 9 September 2019; Accepted 9 September 2019
Available online 09 September 2019

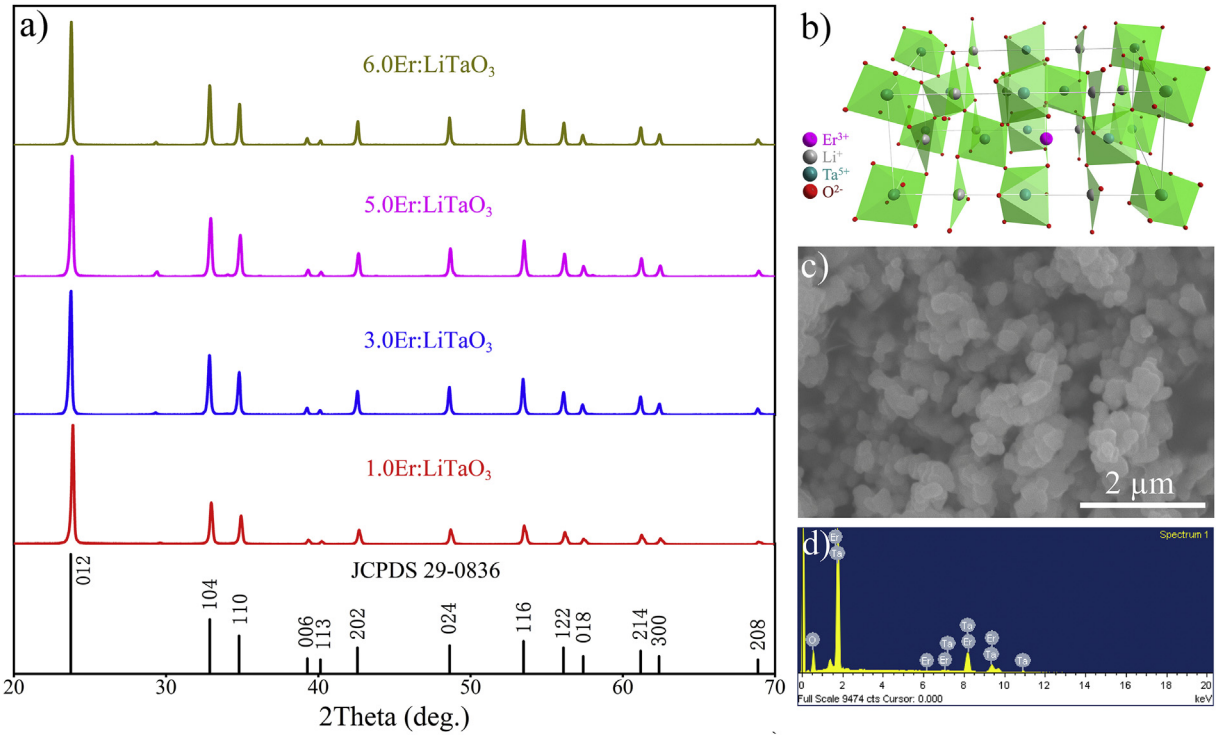

Fig. 1. (a) The XRD patterns for $LiTaO_3$: xEr^{3+} (x = 1.0, 2.0, 3.0, 5.0, 6.0 mol%). (b) The crystal structure of Er^{3+}-doped $LiTaO_3$. (c) The scanning electron microscopic image and (d) the energy dispersive X-Ray spectrum of $LiTaO_3$: $6Er^{3+}$ phosphors.

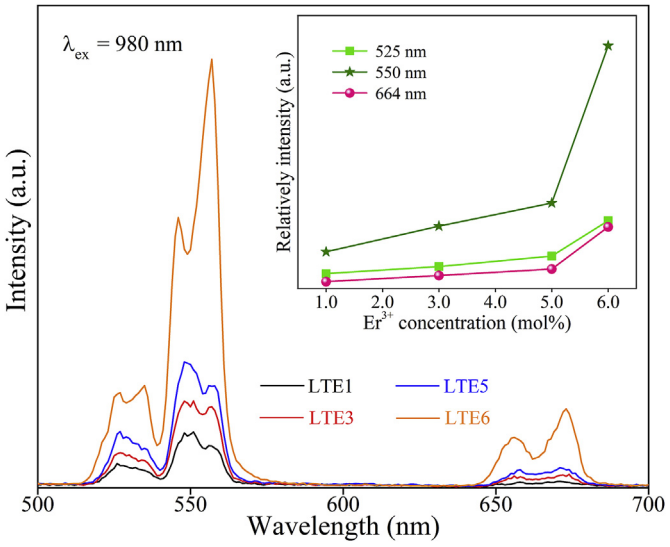

Fig. 2. The emission spectra of Er^{3+}-doped LT excited by 980 nm diode laser, with the concentration dependences of emission intensity at 525 nm, 550 nm and 664 nm shown in the inset.

using molten salt method (MSM). X-ray powder diffraction analysis, morphology characterization, and photoluminescence spectra measurement have been performed on the as-prepared samples. RE-concentration-dependent and power-dependent luminescence spectra were measured, with the possible energy transfer mechanism proposed based on the simplified energy level diagram. Finally, optical temperature sensing properties were investigated by means of FIR method in the temperature range of 100–500 K.

2. Experimental

The $LiTaO_3$:xEr^{3+} (x = 1.0, 3.0, 5.0 and 6.0 mol%) phosphors were synthesized by MSM (henceforth denoted as LTE1, LTE3, LTE5 and LTE6). The starting materials were $LiCO_3$, Ta_2O_5, Er_2O_3, and KCl, purchased from Aladdin Reagent with ultra-purity (99.99%). The raw materials were utilized without further purification. The Li/Ta molar ratio was selected as 1:1 to meet the stoichiometric proportion and thus to eliminate lattice imperfections. The Er^{3+}-doping concentrations were controlled to be 1.0, 3.0, 5.0, and 6.0 mol% in the raw materials, while the KCl/($LiCO_3$ + Ta_2O_5 + Er_2O_3) molar ratio of 20:1 were adopted. The mixture was grounded and ball-milled to uniformity for 30 min and thoroughly mixed for 48 h. Followed, a batch of 15 g mixture was loaded into corundum crucible and transferred to muffle furnace. The target compound powder was preliminary generated by heating the mixture to 850 °C and keeping for 15 min. Finally, the as-grown product was washed with deoxygenated ionized water for 5 times at 80 °C after stirring for 30 min each time to remove the potassium chloride.

The phases of the as-grown powders were characterized by X-ray diffraction (XRD) measurements using an X-ray powder diffractometer (D-Max 2200VPC, Rigaku) with Cu *Kα* radiation (λ = 1.5418 Å) at 40 kV and 30 mA. The morphology, size, and energy dispersive X-Ray (EDX) spectra of the samples were obtained by a field emission scanning electron microscope (FE-SEM, JSM-6330F). The fluorescence emission spectra were recorded using a Photoluminescence Spectrometer (FLS 980, Edinburgh) equipped with a 980 nm semiconductor laser as the excitation source. The temperature dependent UC emission spectra measurement was carried out on the FLS 980 joint with an OptistatDN (Oxford temperature controlling system), which covers a temperature range from 77.5 to 510 K with a precision of ± 0.1 K.

3. Results and discussion

3.1. Structural, phase and morphological analysis

The microscopic structures of the as-prepared $LiTaO_3$:xEr^{3+} samples were determined by comparing their XRD spectra with that from

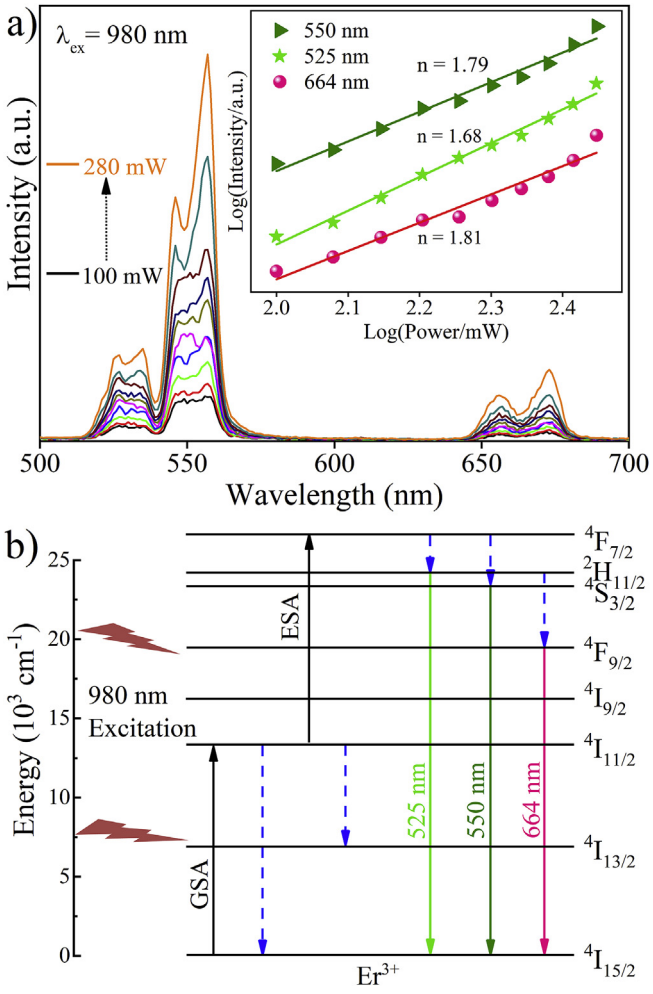

Fig. 3. (a) Power-dependent emission spectra of the $LiTaO_3$:$6Er^{3+}$, with the corresponding Log-Log plots of the power-dependent intensity summarized in the inset. (b) Simplified energy level diagram of Er^{3+} ions doped $LiTaO_3$.

the standard card of pure $LiTaO_3$ (JCPDS 29–0836) as shown in Fig. 1(a). It can be found that the diffraction peaks of the as-prepared samples were well-indexed to lattice planes of pure $LiTaO_3$, indicating that Er^{3+} dopant does not change the crystal structure. Fig. 1(b) illustrates the rhombic crystal structure of Er^{3+}-doped $LiTaO_3$, with the ion Er^{3+} on the Li^+ site. The morphologies of the as-fabricated Er^{3+}-doped LT samples were further examined by SEM, with the image of LT6 depicted in Fig. 1(c) as a representative. The grain sizes are of several hundreds of nanometers, and the particles appear to partly agglomerate, which can be attributed to the inhibition of grain growth caused by the accumulated vacancies on grain boundaries when the Er^{3+} ion with higher valency occupies the Li^+ site [29,30]. The EDX spectrum shown in Fig. 1(d) confirmed that the Er^{3+} ions are doped in the as grown sample and the solvent KCl has been completely removed by the deoxygenated ionized water cleaning process.

3.2. Room-temperature UCL emission

We probed the impact of Er^{3+} doping concentration on optical properties by measuring the UCL emission under 980 nm diode laser excitation at room temperature (Fig. 2). Three up-conversion emission peaks were identified with the centers at 525, 550, and 664 nm in the green and red regions, which can be ascribed to the transitions from $^2H_{11/2}$, $^4S_{3/2}$, and $^4F_{9/2}$ states to $^4I_{15/2}$ state of Er^{3+} ion, respectively [31,32]. Remarkably, for each sample, the emission peak at 550 nm is much higher than the other emission peaks, which will be discussed in details with the multi-photon relaxation mechanism thereafter. As shown in the inset of Fig. 2, the emission intensities at 525, 550, and 664 nm are all enhanced with increasing concentration of Er^{3+} ion from 1.0 to 6.0 mol%, indicating a high tunability of UCL with dopant concentration in the LT system. We speculated that the two green emission bands (centered at 525 and 550 nm) may exhibit strong thermal coupling response due to the suitable energy gap [33], and thus further explored their applications in optical temperature sensing.

To elucidate the energy transfer mechanism in the UCL emission process, we measured the pump power (P) dependent UCL spectra of LTE6 under 980 nm excitation (Fig. 3(a)). The emission intensity was found to monotonically enhance with increasing excitation power from 100 to 280 mW. The relationship between the emission intensity (I_{em}) and the pump laser power (P) of excitation resource can be described as [17]:

$$I_{em} \propto P^n \tag{1}$$

where n is approximately equal to the number of photons absorbed in the UCL process. Accordingly, the emission intensities of $^2H_{11/2} \rightarrow {}^4I_{15/2}$ (green light, centered at 525 nm), $^4S_{3/2} \rightarrow {}^4I_{15/2}$ (green light, centered at 550 nm), and $^4F_{9/2} \rightarrow {}^4I_{15/2}$ (red light, centered at 664 nm) versus the pump power are logarithmically fitted, as presented in the insert of Fig. 3(a). The values of n extracted from the fitting are 1.68, 1.79, and 1.81, respectively, demonstrating two NIR photons are absorbed in the UCL process. The deviation of n from the value of 2.0 can be attributed to the non-radiative processes.

Herein, considering the emission spectra and the power-dependent UCL spectra, a simplified energy level diagram was proposed to depict the up-conversion mechanisms, as shown in Fig. 3(b). Under 980 nm laser excitation, the electron in the ground state ($^4I_{15/2}$) would be excited to the $^4I_{11/2}$ state through the ground state absorption (GSA) mechanism, wherein Er^{3+} ion absorbs a photon, i.e., Er^{3+} ($^4I_{15/2}$) + NIR laser (a photon) → Er^{3+} ($^4I_{11/2}$). The electron at level $^4I_{11/2}$ could then be pumped to the $^4F_{7/2}$ state through the excited state absorption (ESA) processes when excited by another NIR photon. The majority of excited electrons at $^4F_{7/2}$ would relax to $^2H_{11/2}$ and $^4S_{3/2}$ non-radiatively. The green emissions occur when the excited electrons at $^2H_{11/2}$ and $^4S_{3/2}$ relax to $^4I_{15/2}$ ground state with emission peaks of 525 and 550 nm. The red emission centered at 664 nm originates from the non-radiative decay processes from $^4F_{7/2}$, $^4S_{3/2}$ or $^2H_{11/2}$ to $^4F_{9/2}$ states, followed by the transition from $^4F_{9/2}$ to $^4I_{15/2}$ state.

3.3. Temperature sensing properties

In order to evaluate the luminescence temperature sensing properties of $LiTaO_3$:Er^{3+} system, the temperature-dependent UCL emission spectra associated with the thermally coupled energy levels of Er^{3+} ions were recorded at temperatures ranging from 100 to 500 K, as limited by the detection ranges of our equipments. Given the slight difference between the emission intensities under 100 and 120 mW excitations (Fig. 3(a)), the heating effects leading to artificial variation of local temperature become negligible under 100 mW excitation. Therefore, the excitation power of 980 nm laser was set at 100 mW to eliminate possible heating effects as well as to achieve sufficient signal-to-noise ratio. As shown in Fig. 4, the intensity of green emission (centered at 550 nm) substantially drops with rising temperature, which can be ascribed to the intense thermal quenching at high temperature that prevents electrons from relaxing to the $^4S_{3/2}$ level [34,35]. According to the Boltzmann distribution among the $^2H_{11/2}$ and $^4S_{3/2}$ energy levels, the FIR can be expressed as:

$$R = \frac{I_{525}}{I_{550}} = C \times \exp\left(-\frac{\Delta E}{kT}\right) \tag{2}$$

where I_{525} and I_{550} are the integrated intensities of the $^2H_{11/2} \rightarrow {}^4I_{15/2}$ and $^4S_{3/2} \rightarrow {}^4I_{15/2}$ transitions, C is a constant, k is the Boltzmann constant, T is the absolute temperature, ΔE is the energy gap between the

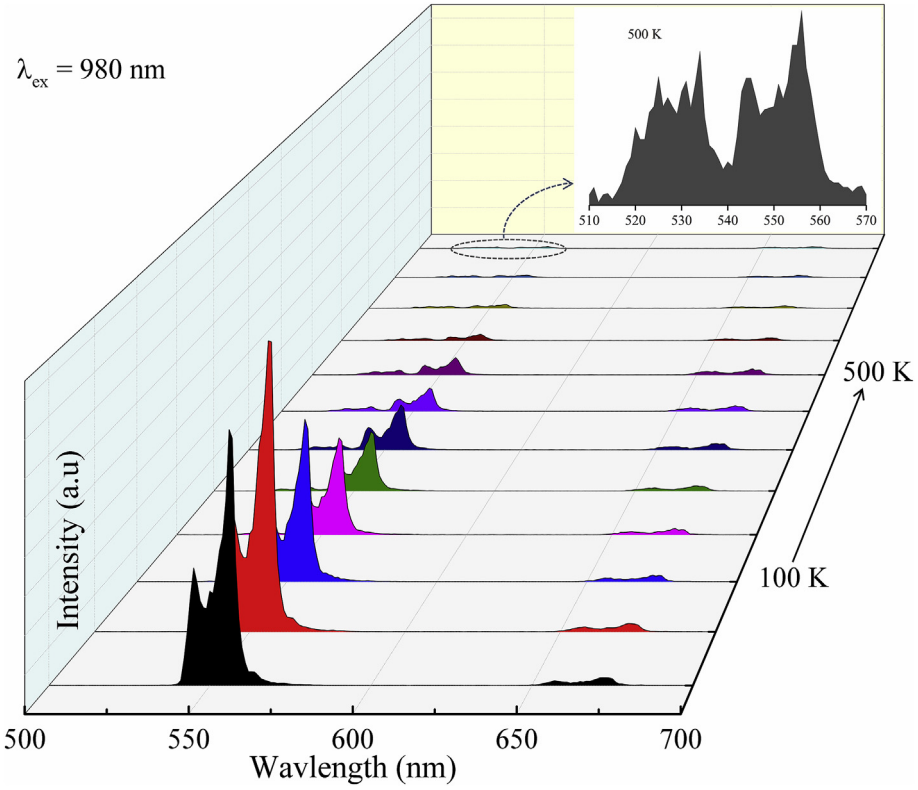

Fig. 4. Temperature dependent emission spectra of $LiTaO_3:6Er^{3+}$ at 100–500 K. The inset presents the partial enlarged view at 500 K.

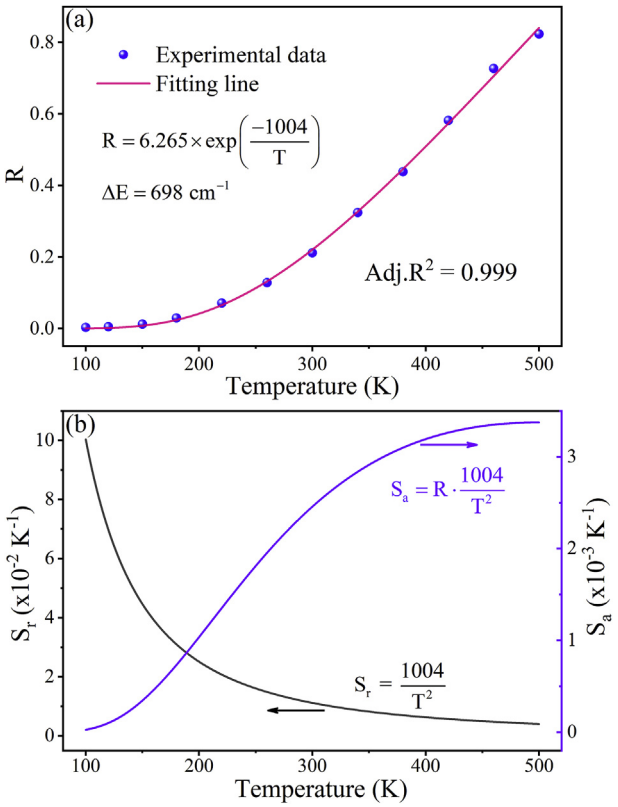

Fig. 5. (a) Fluorescence intensity ratio of $LiTaO_3:6Er^{3+}$ sample in the range of 100–500 K and the fitting result by the equation FIR = C × exp(-ΔE/k_B/T). (b) Absolute sensitivity S_a and relative sensitivity S_r of $LiTaO_3:6Er^{3+}$ sample as the functions of temperature.

$^2H_{11/2}$ and $^4S_{3/2}$ levels.

As shown in Fig. 5(a), R as a function of temperature measured in experiments can be well fitted using Eq. (2) with the adjusted R-Square of 0.999, verifying that the temperature dependence of R originates from the thermal coupling between adjacent energy levels. In the high temperature range of 300–500 K, R exhibits great linearity to temperature, because of the non-radiative relaxation and the energy transfer between the matrix and Er^{3+} ions [36]. The constant C and the effective energy gap ΔE are determined to be 6.265 and 698 cm^{-1}, respectively. Compared with other reported studies as listed in Table 1, the value of ΔE is larger than those of most Er^{3+} ion doped fluoride phosphors crystal [13], oxide crystal [14], and ceramic systems, despite being slightly lower than the values for ceramics containing Na-$LaMgWO_6$ [37], Y_2O_3 [38], and $Na_{0.5}Bi_{0.5}TiO_3$ [39]. It is worth noting that the energy gap between thermally coupled levels should be lower than 2000 cm^{-1} to enable non-trivial population of the upper level for harnessing thermal coupling effect, while higher than 200 cm^{-1} to avoid the overlap of two emissions bands [40]. Therefore, the intrinsic energy gap of the $LiTaO_3:Er^{3+}$ material is suitable for applications in optical thermometry.

The absolute sensitivity (S_a) and relative sensitivity (S_r), serving as the key figure-of-merit of optical temperature sensors materials, were derived from Eq. (2) as:

$$S_a = \left|\frac{d(R)}{dT}\right| = R\cdot\left(\frac{\Delta E}{kT^2}\right) \quad (3)$$

$$S_r = \left|\frac{1}{R}\frac{d(R)}{dT}\right| = \frac{\Delta E}{kT^2} \quad (4)$$

The absolute and relative sensitivities of the sample LTE6 in the temperature range of 100–500 K were calculated using Eq. (3) and Eq. (4), with the fitted function of R based on experimental FIR data. As presented in Fig. 5(b), S_a nonlinearly increases with increasing temperature, with the maximum value of 3.34 × 10^{-3} K^{-1} obtained at 492 K, which is better than the performance of Er^{3+} doped materials reported

Table 1
The optical temperature sensing parameters of RE^{3+}-doped materials with different matrices.

System	T-range (K)	ΔE (cm^{-1})	S_a ($10^{-3}K^{-1}$)	Ref.
Er:BNT-KNN	293–473	546	2.2	[8]
Er:BiOCl	298–778	864	2.8	[12]
Er:Yb:LaF_3	300–515	549	1.57	[13]
Er:Yb:$CaWO_4$	300–540	658	3	[14]
Er:$LiTaO_3$	100–500	698	3.34	This work

previously [8,12–14]. By contrast, S_r sharply decreases with increasing temperature in the low temperature range, and flattens out in the high temperature range. The results suggest that the $LiTaO_3$:Er^{3+} material can be applied to luminescence temperature sensing in a wide temperature range.

4. Conclusion

A series of Er^{3+}-doped lithium tantalate phosphors have been synthesized by molten salt method. The tunability of emission intensity via the control of Er^{3+} doping concentration was demonstrated by room temperature UCL spectra. Two-photon absorption process was confirmed by the analysis of the pump power dependent UCL spectra, with the underlying mechanism proposed based on an energy level diagram. The optical temperature sensing performance of the Er^{3+}:$LiTaO_3$ matrix was evaluated for the thermal coupling energy levels of $^2H_{11/2}$ and $^4S_{3/2}$, resulting in the ΔE of 698 cm^{-1} and the maximal S_a of 3.34×10^{-3} K^{-1} at 492 K. The relatively high sensitivity and wide operation scope of Er^{3+}:$LiTaO_3$ observed in this study, as well as the indispensable role of the $LiTaO_3$ matrix in the area of integrated optics, reveals the great potential to harness the merits of both dopant and matrix to develop wide temperature range integratable optical thermometry.

Acknowledgments

This work was supported by National Natural Science Foundation of China (NSFC) (No. 11832019, 11804403, 11372361), Guangdong Science & Technology Project (2015B090927005), Guangdong Natural Science Funds for Distinguished young scholar (2018B030306036), and Natural Science Foundation of Guangdong Province (2018A030313909).

References

[1] G. Gao, D. Busko, S. Kauffmann-Weiss, A. Turshatov, I.A. Howard, B.S. Richards, Wide-range non-contact fluorescence intensity ratio thermometer based on Yb^{3+}/Nd^{3+} co-doped La_2O_3 microcrystals operating from 290 to 1230 K, J. Mater. Chem. C 6 (2018) 4163–4170.
[2] M. Quintanilla, L.M. Liz-Marzán, Guiding rules for selecting a nanothermometer, Nano Today 19 (2018) 126–145.
[3] Y. Tu, S. Zhao, D. He, T. Wu, H. Zhang, R. Lei, L. Huang, S. Xu, A portable all-fiber thermometer based on the fluorescence intensity ratio (FIR) technique in rare earth doped TeO_2–WO_3–La_2O_3–Na_2O glass, J. Mater. Chem. C 6 (2018) 7063–7069.
[4] F. Vetrone, R. Naccache, A. Zamarrón, A. Juarranz de la Fuente, F. Sanz-Rodríguez, L. Martinez Maestro, E. Martín Rodriguez, D. Jaque, J. García Solé, J.A. Capobianco, Temperature sensing using fluorescent nanothermometers, ACS Nano 4 (2010) 3254–3258.
[5] F. Huang, Y. Gao, J. Zhou, J. Xu, Y. Wang, Yb^{3+}/Er^{3+} co-doped $CaMoO_4$: a promising green upconversion phosphor for optical temperature sensing, J. Alloy. Comp. 639 (2015) 325–329.
[6] H. Kusama, O.J. Sovers, T. Yoshioka, Line shift method for phosphor temperature measurements, Jpn. J. Appl. Phys. 15 (1976) 2349–2358.
[7] X. Chai, J. Li, X. Wang, Y. Li, X. Yao, Color-tunable upconversion photoluminescence and highly performed optical temperature sensing in Er^{3+}/Yb^{3+} co-doped $ZnWO_4$, Opt. Express 24 (2016) 22438–22447.
[8] X. Jia, J. Zhang, Y. Gao, J. Wang, P. Zheng, Enhanced bipolar fatigue-resistance and optical temperature sensing in Er-modified $0.94(Bi_{0.5}Na_{0.5})TiO_3$-$0.06(K_{0.5}Na_{0.5})NbO_3$ lead-free ceramics, Mater. Res. Bull. 89 (2017) 11–15.
[9] J. Zhou, Y. Chen, R. Lei, H. Wang, Q. Zhu, X. Wang, Y. Wu, Q. Yang, S. Xu, Excellent photoluminescence and temperature sensing properties in Ho^{3+}/Yb^{3+} codoped $(Y_{0.88}La_{0.09}Zr_{0.03})_2O_3$ transparent ceramics, Ceram. Int. 45 (2019) 7696–7702.
[10] Z. Sun, G. Liu, Z. Fu, Z. Hao, J. Zhang, A novel upconversion luminescent material: Li^+- or Mg^{2+}-codoped $Bi_{3.84}W_{0.16}O_{6.24}$:$Tm^{3+}$, Yb^{3+} phosphors and their temperature sensing properties, Dyes Pigments 151 (2018) 287–295.
[11] H. Yu, Y. Li, Y. Song, Y. Wu, X. Lan, S. Liu, Y. Tang, S. Xu, B. Chen, Ultralong well-aligned TiO_2:Ln^{3+} (Ln = Eu, Sm, or Er) fibres prepared by modified electrospinning and their temperature-dependent luminescence, Sci. Rep. 7 (2017) 44099.
[12] P. Du, L. Luo, J.S. Yu, Tunable color upconverison emissions in erbium(III)-doped BiOCl microplates for simultaneous thermometry and optical heating, Microchim. Acta 184 (2017) 2661–2669.
[13] X. Cheng, X. Ma, H. Zhang, Y. Ren, K. Zhu, Optical temperature sensing properties of Yb^{3+}/Er^{3+} codoped LaF_3 upconversion phosphor, Physica B 521 (2017) 270–274.
[14] X. Cheng, K. Yang, J. Wang, L. Yang, X. Cheng, Up-conversion luminescence and optical temperature sensing behaviour of Yb^{3+}/Er^{3+} codoped $CaWO_4$ material, Opt. Mater. 58 (2016) 449–453.
[15] X. Li, J. Cao, Y. Wei, Z. Yang, H. Guo, Optical thermometry based on up-conversion luminescence behavior of Er^{3+}-doped transparent Sr_2YbF_7 glass-ceramics, J. Am. Ceram. Soc. 98 (2015) 3824–3830.
[16] H. Zhang, D. Peng, W. Wang, L. Dong, C. Pan, Mechanically induced light emission and infrared-laser-induced upconversion in the Er-doped CaZnOS multifunctional piezoelectric semiconductor for optical pressure and temperature sensing, J. Phys. Chem. C 119 (2015) 28136–28142.
[17] C.R. Li, B. Dong, C.G. Ming, M.K. Lei, Application to temperature sensor based on green up-conversion of Er^{3+} doped silicate glass, Sensors 7 (2007) 2652–2659.
[18] W.A. Pisarski, J. Pisarska, R. Lisiecki, W. Ryba-Romanowski, Er^{3+}/Yb^{3+} co-doped lead germanate glasses for up-conversion luminescence temperature sensors, Sensor. Actuat. A-Phys 252 (2016) 54–58.
[19] B. Dong, T. Yang, M.K. Lei, Optical high temperature sensor based on green up-conversion emissions in Er^{3+} doped Al_2O_3, Sens. Actuators B Chem. 123 (2007) 667–670.
[20] X. Wang, X. Kong, Y. Yu, Y. Sun, H. Zhang, Effect of annealing on upconversion luminescence of ZnO:Er^{3+} nanocrystals and high thermal sensitivity, J. Phys. Chem. C 111 (2007) 15119–15124.
[21] E. Cortés-Adasme, M. Vega, I.R. Martin, J. Llanos, Synthesis and characterization of $SrSnO_3$ doped with Er^{3+} for up-conversion luminescence temperature sensors, RSC Adv. 7 (2017) 46796–46802.
[22] D. Psaltis, S.R. Quake, C. Yang, Developing optofluidic technology through the fusion of microfluidics and optics, Nature 442 (2006) 381–386.
[23] K.S. Abedin, T. Tsuritani, M. Sato, H. Ito, Integrated intracavity quasi-phase-matched second harmonic generation based on periodically poled Nd:$LiTaO_3$, Appl. Phys. Lett. 70 (1997) 10–12.
[24] V.Y. Shur, A.R. Akhmatkhanov, D.S. Chezganov, A.I. Lobov, I.S. Baturin, M.M. Smirnov, Shape of isolated domains in lithium tantalate single crystals at elevated temperatures, Appl. Phys. Lett. 103 (2013) 242903.
[25] X.F. Yang, C.Y. Zhang, Z.B. Zhang, E.Y.B. Pun, D.L. Zhang, Low-loss Ga:Er:$LiTaO_3$ optical waveguide for integrated optics, Mater. Lett. 227 (2018) 199–201.
[26] X. Yang, Y. Zhu, D. Ma, S. Long, Z. Liu, B. Wang, Luminescent properties of stoichiometric Er:$LiTaO_3$ submicron particles synthesized by a modified solid-state combustion route, Ceram. Int. 45 (2019) 10733–10739.
[27] G. Gasparotto, S.A.M. Lima, M.R. Davolos, J.A. Varela, E. Longo, M.A. Zaghete, Luminescence properties of Eu^{3+}- and Mg^{2+}-doped $LiTaO_3$ obtained via the polymeric precursor method, J. Lumin. 128 (2008) 1606–1610.
[28] X. He, K. Li, M. Liu, Y. He, X. Zhang, Y. Zhao, D. Xue, An optical spectroscopy study of defects in lithium tantalate single crystals, Opt. Commun. 281 (2008) 2531–2534.
[29] D. Gao, K.W. Kwok, D. Lin, H.L.W. Chan, Microstructure and electrical properties of La-modified $K_{0.5}Na_{0.5}NbO_3$ lead-free piezoelectric ceramics, J. Phys. D Appl. Phys. 42 (2008) 035411.
[30] J. Lin, J. Xu, C. Liu, Y. Lin, X. Wu, C. Lin, X. Zheng, C. Chen, Effects of compositional changes on up-conversion photoluminescence and electrical properties of lead-free Er-doped $K_{0.5}Na_{0.5}NbO_3$-$SrTiO_3$ transparent ceramics, J. Alloy. Comp. 784 (2019) 60–67.
[31] P. Liu, F. Wang, X. Chen, B. Yang, Upconversion/Downconversion luminescence and preparation of NIR-to-UV-excited Gd_2O_2S:Er phosphor, J. Lumin. 200 (2018) 126–132.
[32] M. Hirano, K. Ishikawa, Hydrothermal formation and up-conversion luminescence of Er^{3+}-doped $GdNbO_4$, J. Am. Ceram. Soc. 100 (2017) 2814–2821.
[33] M. Pollnau, D.R. Gamelin, S.R. Lüthi, H.U. Gudel, M.P. Hehlen, Power dependence of upconversion luminescence in lanthanide and transition-metal-ion systems, Phys. Rev. B 61 (2000) 3337–3346.
[34] W.A. Pisarski, J. Janek, J. Pisarska, R. Lisiecki, W. Ryba-Romanowski, Influence of temperature on up-conversion luminescence in Er^{3+}/Yb^{3+} doubly doped lead-free fluorogermanate glasses for optical sensing, Sens. Actuators B Chem. 253 (2017) 85–91.
[35] N. Vijaya, P. Babu, V. Venkatramu, C.K. Jayasankar, S.F. León-Luis, U.R. Rodríguez-Mendoza, I.R. Martín, V. Lavín, Optical characterization of Er^{3+}-doped zinc fluorophosphate glasses for optical temperature sensors, Sens. Actuators B Chem. 186 (2013) 156–164.
[36] X. Wang, Q. Liu, P. Cai, J. Wang, L. Qin, T. Vu, H.J. Seo, Excitation powder dependent optical temperature behavior of Er^{3+} doped transparent $Sr_{0.69}La_{0.31}F_{2.31}$ glass ceramics, Opt. Express 24 (2016) 17792–17804.
[37] J. Zhang, C. Jin, Electronic structure, upconversion luminescence and optical temperature sensing behavior of Yb^{3+}-Er^{3+}/Ho^{3+} doped $NaLaMgWO_6$, J. Alloy. Comp. 783 (2019) 84–94.
[38] V.K. Rai, A. Pandey, R. Dey, Photoluminescence study of Y_2O_3:Er^{3+}-Eu^{3+}-Yb^{3+} phosphor for lighting and sensing applications, J. Appl. Phys. 113 (2013) 083104.
[39] P. Du, J. Su Yu, Effect of molybdenum on upconversion emission and temperature sensing properties in $Na_{0.5}Bi_{0.5}TiO_3$:Er/Yb ceramics, Ceram. Int. 41 (2015) 6710–6714.
[40] J. Zhang, Y. Zhang, X. Jiang, Investigations on upconversion luminescence of $K_3Y(PO_4)_2$:Yb^{3+}-Er^{3+}/Ho^{3+}/Tm^{3+} phosphors for optical temperature sensing, J. Alloy. Comp. 748 (2018) 438–445.